Automated Detection of Power Quality Disturbances using none subsampled Contourlet Transform & Multiclass Support Vector Machine

[1]Deepti Priyanka Behera, [1] A.K.Pradhan[1]Ashis Kumar Mallick [1] Jyoti Prakash, [1] Girija Sankar Dora

[1]Asst. Prof. Department of Electrical & Electronics Engineering, GITAM BHUBANESWAR ODISHA

Abstract: The Nonsubsampled Contourlet Transform NSCT is a signal processing technique that offers a flexible way to decompose signals, particularly for analyzing power quality events. Here's a breakdown of the key points from your description:The NSCT is built on a non-subsampled pyramid structure and nonsubsampled directional filter banks. This allows for multiscale, multidirectional of detail.NSCT is designed to provide better frequency selectivity and regularity compared to traditional methods like the Contourlet Transform. This makes it well-suited for analyzing power quality disturbances with varying frequencies.The paper proposes a design framework based on a mapping approach, which enables fast feature extraction from power quality events. This reduces the computational complexity of the transformation process.The paper introduces a signal decomposition method that separates signals into oscillatory and transient components using theNSCT. Thehigh-frequency subbands of the NSCT coefficients are the focus on fusion scheme to separate the oscillatory component.Low-frequency coefficients are fused by taking the average of the corresponding coefficients from the input signal to capture the transient signal

Keywords: Signal processing,Nonsubsampled Contourlet Wavelet Transform (NCT),MCA, SALSA, Multi Class support vector machines, power quality disturbances

Introduction

Power quality (PQ) refers to the characteristics of the electrical power supply that affect the performance of connected electrical and electronic equipment [1]. With the proliferation of electronic devices, fast control equipment, and renewable energy sources in the power system, maintaining a high-quality power supply has become increasingly important. PQ disturbances [2] can be broadly categorized into two types: transient and steady-state disturbances. Transient disturbances are short-duration events, such as voltage sags (momentary drops in voltage), swells (momentary increases in voltage), interruptions (complete loss of voltage), and transients (rapid and short-term voltage variations). On the other hand, steady-state disturbances are continuous issues, such asharmonics (additional frequency components on top of the fundamental frequency) and voltage fluctuations (small variations in voltage over time) [3-9].The integration of renewable energy sources, such as solar and wind, can introduce additional challenges to power quality due to their intermittent nature. Moreover, the presence of various PQ disturbances in the power system can lead to simultaneous occurrences of two or more disturbances, making the detection and mitigation of these issues more complex[10-13]. The present paper presents a novel Multimodal MIF (Modality Independent Fusion) method that is based on the NSCT (Nonsubsampled Contourlet Transform) domain. The proposed method utilizes a statistical approach to fuse coefficients from different subbands in NSCT. This paper introduces a new method for Multimodal MIF that takes advantage of the NSCT domain. NSCT is a transform used for image and signal processing that can effectively capture various directional and scale information, making it suitable for handling multimodal data. The proposed method utilizes the Generalized Gaussian Density to fit the marginal distributions of the high-frequency coefficients. Generalized Gaussian Density (GGD) is a flexible probability distribution that can model a wide range of data, making it suitable for various applications.

The feature extraction process plays a critical role as the overall recognition accuracy depends not only on the choice of the classifier but also on the quality and relevance of the features extracted.

, and shift-invariant signal decomposition.The non-subsampled version ensures that the signal decomposition is shift-invariant, which means it's effective at detecting features of power quality disturbances across different time shifts.A pyramid structure is used for hierarchical representation of the signal with multiple scales. This is beneficial for capturing features at different levels

reconstruction condition. This means that after decomposition and reconstruction, the output signal is nearly identical to the original input signal. To move to the next level of decomposition, all filters are upsampled by a factor of 2 in both dimensions. This process allows for capturing information at finer scales. Filtering with the upsampled filters is as complex as filtering with the original filters using the 'à trous' algorithm. The 'à trous' algorithm is an efficient wavelet decomposition technique. The analysis part of the nonsubsampled pyramid is cascaded to achieve the multiscale decomposition. Cascading involves connecting the output of one analysis block to the input of the next, creating a series of filters for multiscale decomposition. The equivalent filters for a k-th level cascading nonsubsampled pyramid are specified, but the exact details are not provided in the excerpt. These filters are essential for performing the cascading operation correctly.

The Proposed Signal Fusion Technique

Fusion of the High Frequency Coefficients:

High-frequency subbands in an image generally contain detailed information like edges, lines, and corners. These regions contribute to the fine details and structures in the image [33]. But in case of signal Different signaling modalities often contain overlapping and unique information about the same scene or subject.The selection rule aims to capture the most important information from source images for effective fusion. In this fusion scheme is introduced for high-frequency subbands.Weight maps, which indicate the importance of coefficients, are proposed for guiding the fusion process. These weight maps are determined based on saliency maps.The Nonsubsampled Contourlet Transform (NSCT) coefficients exhibit dependencies due to their multiscale and multidirectional nature.The dependencies between high-frequency coefficients from different NSCT subbands are used to update and enhance the coefficients.The proposed process involves updating the high-frequency coefficients based on the relationships between NSCT subbands.After updating, the coefficients are combined using the weight maps, which guide the fusion process by assigning different levels of importance to different coefficients.

This fusion approach aims to enhance the fused image by capturing both fine details and overall complexity.It's important to note that the exact implementation of the fusion rule and the specific parameters chosen will influence the results. This method attempts to strike a balance between preserving important details and avoiding artifacts, and its effectiveness will depend on the nature of the source images and the fusion task.

Nonsubsampled Contourlet Wavelet Transform - based Signal Decomposition Technique

The nonsubsampled pyramids (NSP) and directional filter bank (NSDFB) stages make up the NSCT decomposition process. The former decomposes multiscale, whereas the latter decomposes directionally. Each level of the NSP separates picture into low- and high-frequency sub bands. NSP generates k+1 sub band pictures, one low-frequency and k high-frequency, with a decomposition level of k. NSDFB decomposes NSP high-frequency sub bands at each level. For a given sub band, l decomposition directions provide 2l directional sub bands with the same size as the original picture. After repeatedly decomposing the low frequency component, an image is divided into one low frequency sub signal and a sequence of high frequency directional sub band signal tures (k j=1 2lj), where lj is the number of decomposition directions at the j scale.Fig. 1 is representing the pyramid structure of NCT.

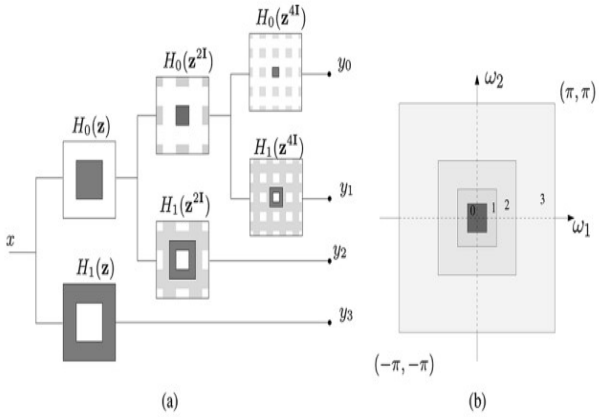

Fig.1: Block diagram of NCT of an input signal x[n] using NCT

The NCT algorithm decomposes the input signal into subbands using a series of low-pass and high-pass filters. Each level of decomposition splits the signal into two subbands, representing different frequency ranges. The low-pass subband captures the lower frequencies, while the high-pass subband contains the higher frequencies or details.By applying the NCT recursively up to the desired level, a multilevel representation of the input signal is obtained. The constraints on α and β, along with the proper design of the filters' frequency responses, ensure that the decomposition and subsequent reconstruction can be performed accurately, preserving the signal's characteristics without introducing redundancy.

This involves repeatedly applying nonsubsampled filter banks to achieve the desired level of decomposition. The filters used in the construction satisfy the perfect

Where the parameter a is a constant, which tunes the sharpness of fused image by adjusting the value of parameter; it is set to 1.2 in our experiment.

Fusion For Low Frequency

Let $C_0^{\lambda}(x,y)$denote the low frequency subband coefficient at location (x,y); λ is input image A, *B.* Finally, the fused image can be obtained by

$$C_0^{\lambda}(x,y) = \sum_{\lambda=A,B} [\delta_{\lambda} C_0^{\lambda}(x,y) + \xi_{\lambda} C_0^{\lambda}(x,y)]$$

High-frequency subbands capture detailed information like edges, lines, and corners. The goal of this process is to capture salient information from different imaging

$$E_{\lambda}(x,y) = \frac{1}{|R|} \sum_{i.j} \left(C_0^{\lambda}(i,j)\right)^2 \log\left(C_0^{\lambda}(i,j)\right)^2$$

(2)

Computing the weights $(\delta_{\lambda}, \xi_{\lambda})$ of the standard deviation$D_{\lambda}(x,y)$and the information entropy $E_{\lambda}(x,y)$respectively,

$$\delta_{\lambda} = \frac{|D_{\lambda}(x,y)|^{\alpha}}{|D_A(x,y)|^{\alpha} + |D_B(x,y)|^{\alpha}} ;$$

$$\xi_{\lambda} = \frac{E_{\lambda}(x,y)}{E_A(x,y)+E_B(x,y)}$$

modalities and enhance the overall fusion performance.Updating of the High Frequency Subband Coefficients. First, we calculate the horizontal dependency$\mathrm{jsd}_{\mathrm{l},\theta,\mathrm{h}}$ between coefficients with different directions at the same scale las

$$js_{\ l,\theta,h}(x,y) = \sum_{j=1.j\#i}^{K} D_{JS}\left(C_{l,\theta_i}(x,y), C_{l,\theta_j}(x,y)\right)$$

(5)

Where $K$is the total of the subbands at the$l$th scale.

Then we calculate the vertical dependency $jsd_{i,\theta,v}$between the specified subband's (for instance subband$i$)parents and children

. Computing the regional standard deviation $D_{\lambda}(x,y)$

$$D_{\lambda}(x,y) = \sqrt{\sum_{m\epsilon M, n\epsilon N} \omega(m,n) \times [C_{\lambda}(x+m, y+n) - S_{\lambda}(x,y)]^2}$$

(1)

Calculating the normalized Shannon entropy

$$jsd_{l,\theta,v}(x,y) = \sum_{j=1}^{K} D_{JS}\left(C_{l,\theta_i}(x,y), C_{l-1,\theta_j}(x,y)\right) + D_{JS}\left(C_{l,\theta_i}(x,y), C_{l+1,\theta_j}(x,y)\right)$$

(6)

Further, the horizontal and vertical dependency components are normalized, respectively,

$$jsd_{l,\theta,h}(x,y) = \frac{jsd_{l,\theta,h}(x,y)}{jsd_{l,\theta,h}(x,y)+jsd_{l,\theta,v}(x,y)}, jsd_{l,\theta,v}(x,y) = \frac{js_{\ l,\theta,v}(x,y)}{jsd_{l,\theta,h}(x,y)+jsd_{l,\theta,v}(x,y)}$$

(7)

Finally, the high frequency NSCT coefficients are revised as

$$C_{l,\theta}(x,y) = C_{l,\theta}(x,y)\sqrt{1 + jsd_{l,\theta,h}(x,y)^2 + jsd_{l,\theta,v}(x,y)^2}$$

(8)

The process of constructing weight maps using saliency information and applying a Gaussian filter to each high-pass subband. These weight maps play a crucial role in guiding the fusion algorithm for achieving an informative and balanced fused signal. By assigning appropriate weights to different parts of the subband coefficients based on their saliency levels, the fusion process is enhanced and prioritizes significant elements such as edges and corners.

$$S_{l,\theta}(x,y) = \left|C_{l,\theta}(x,y)\right| * g_{r_g,\theta_g}(x,y)$$

(9)

for their unique properties and the variations caused by the decomposition process.

y =[y(J^{l}_{s} , n), y2(2, n), ⋯ y(J^{h}_{s} , n)] $^{T}\in$ R(J^{h}_{s} −J^{l} s +1)×^{N} (14)

E_y(j, n)= ||Hilbert(y(j, n))||$_2$, $J^{l}_{s} \le j \le J^{h}_{s}$ 15)

We acquire the frequency domain sequence FE(j,) by performing the M-point discrete Fourier transform (DFT) on Ey(j, n), and from this we can derive the power spectrum P_E(j,) of the layer j signal envelope.P_E(j, ω)=$\frac{F_E(j,w).F_E^*(j,w)}{M}$

(16)

In this case, the Power Spectrum Kurtosis (PSK) is defined as the complex conjugate of the power spectrum (F_E*(j, ω)).

$$PSK(j)=\frac{\frac{1}{M/2}\sum_{i=1}^{M/2}\left[P_E(j,w)-\overline{P_E(j,w)}\right]^4}{\left[\frac{1}{M/2}\sum_{i=1}^{M/2}\left[P_E(j,w)-\overline{P_E(j,w)}\right]^2\right]^2}$$

(17)

Based on Fig.2, it is observed that the value of SAEWAE (presumably an evaluation metric) is the lowest among the presented options with respect to GCD and JSD. Therefore, in this method, these specific values of Q=3 and r=3 are selected as the optimal parameter values coefficient plot of signal before and after proposed algorithm (b) Adaptive parameter optimization for PQ Disturbances as a three-dimensional curve. we can see the SAEWSE value in the two-dimensional grid search space of parameters and based on the minimum SAEWSE curve value, we can determine the optimal parameters in NCT.

Selection of parameters

The study suggests a technique for splitting a signal into its oscillatory and transient parts. Sparse representations of these parts are achieved by employing the tδ_λ and $\xi_\lambda$value in NCT in this method. The oscillatory component is represented by the high δ_λ and $\xi_\lambda$value in NCT NCT, while the transient component is modeled by the low $\delta_\lambda$and $\xi_\lambda$value in NCT. Oscillatory and transient

Where $g(\cdot)$is a Gaussian low pass filter, whose size is $(2r_g + 1) \times (2r_g + 1)$, and the parameters $r_g$and $\theta_g$are set to 5. Next, the weight maps are determined by comparison of the saliency maps $\left(S^n_{l,\theta}(x,y), n \in [A,B]\right)$

$$W^n_{l,\theta}(x,y) = \begin{cases} 1 \ if \ (S^n_{l,\theta}(x,y) = \max\left(S^A_{l,\theta}(x,y), S^B_{l,\theta}(x,y)\right) \\ 0 \ \text{otherwise} \end{cases}$$

(10)

Finally, the fused subband coefficients $C^F_{l,\theta}(x,y)$can be obtained by the weighted summation

$$C^F_{l,\theta}(x,y) = W^A_{l,\theta}(x,y)C^A_{l,\theta}(x,y) + W^B_{l,\theta}(x,y)C^B_{l,\theta}(x,y)$$

(11)

Determination of Energy to capture the features

The challenges associated with evaluating the sparsity of wavelet coefficients obtained through the Non-Subsampled Contourlet Transform (NSCT) decomposition. Unlike traditional wavelet transforms, NSCT employs a two-channel bandpass filter for iterative signal decomposition, resulting in a sequence of wavelet coefficients that can vary in length. This poses difficulties when using traditional measures like Shannon entropy to evaluate sparsity accurately. The value called "SAEWSE" to address this issue.

$$p^{(j)}_i=\frac{E_\lambda(x,y)/\ Nj\ |w(j)}{\sum_{j=1}^{j+1}\sum_{i=1}^{N_j}\frac{E_j}{N_j}\left|w_i^j\right|}$$

(12)

$$SAEWSE = -\sum_{j=1}^{J+1}\sum_{i=1}^{N_j} p_i^{(j)} ln\, p_i^{(j)}$$

(13)

where Ej, Nj, and w(j) I represent the NSCT energy which are represented in equation (11), length of the sequence and coefficients of wavelets respectively up to of the jth layer.To address this challenge, it appears that a different measure called "SAEWSE" (which stands for something not mentioned in your text) is introduced.

This measure might be designed specifically to evaluate the sparsity of NSCT coefficients in a way that accounts

SALSA's approach of iteratively updating variables while considering constraints makes it suitable for solving the optimization problem you've described.The underlying principle of the algorithm is the following minimization problem. The generic version of the unbounded optimization issue described in (14) is as follows:

Even when wavelets have the same , their waveforms can vary significantly across different subbands. The δ_λ and $\xi_\lambda$value in NCT alone does not determine the specific shape or characteristics of the wavelet waveform in each subband. Other factors, such as the specific subband frequencies and filter characteristics, can influence the shape and properties of the wavelet waveforms.

Choise of MotherWavelet

The provided information suggests that an algorithm based on Minimum Description Length (MDL) has been utilized to select the appropriate decomposition level and mother wavelet for fault voltage signal analysis. Table 1 presents the results of the algorithm, indicating the MDL values for different levels and wavelets.Based on the MDL values shown in Table 1, it is determined that the minimum MDL value of -100.19 is achieved at level 3 with the Bior 4.4. For the decomposition at level 3 with the Bior 4.4, the chosen δ_λ and $\xi_\lambda$value in NCT value is 3. These parameter selections are illustrated in Fig.3. In this case, the fundamental component with a frequency of 50 Hz is of particular importance in choosing the appropriate parameters for different power quality disturbance signals. It's important to note that the specific details and rationale behind the algorithm, MDL computation, wavelet selection, and the impact of δ_λ and $\xi_\lambda$value in NCTvalues require further information or reference to Table 1 and Fig.4 to provide more specific insights.

Algorithm for parameter selection in NCT

components may be effectively separated using morphological component analysis (MCA) because to the limited coherence between low and high δ_λ and $\xi_\lambda$value in NCT.

In this study, the split augmented Lagrangian shrinkage method (SALSA) [30] is used to address the MCA-related optimization problem. By repeatedly updating the oscillatory and transient components, this technique makes it easier to decompose the signal.

The ability to encode distinct frequency and temporal characteristics in different subbands allows for a more comprehensive representation of signal components. This approach efficiently captures and separates oscillatory and transient features, and parameter selection aims to strike a balance between computational efficiency and accurate decomposition.The values of δ_λ and $\xi_\lambda$value in NCT are then fine-tuned to achieve the desired frequency decomposition.

If X is the signal then signal is devided into high and low oscillatory components. The objective of MCA is to find out X_1 and X_2separately.Where X_1 and X_2 are the sparse representation of the matrix. X_1 is sparsely represented by NCT_1 with JSD. Trnasformation matrix is denoted by φ_1. Simirly X_2 is sparsely represented by NCT_2 with parameters of different JSD. Trnasformation matrix is denoted by φ_2.

$$X = X_1 + X_2 \tag{18}$$

$$\{W_1^{opt}, W_2^{opt}\} = \underset{w_1\ w_2}{\operatorname{argmin}} \| W_1 \|_1 + \| W_2 \|_1$$

SALSA

Minimizing the objective function in the context of signal decomposition with sparsity constraints is discussed here [14-15]. To address these challenges, you've chosen to use the Split Augmented Lagrangian Shrinkage Algorithm (SALSA), a specialized optimization method designed to handle non-smooth and constrained optimization problems efficiently.

variance at individual points on the grid is not displayed on the surface map.

These graphs are helpful in feature extraction because they show how a dependent variable, and two independent variables are related to one another. By plotting $f_1(W)$, $f_2(W)$ and U we can get the features of different power quality events which are

Kurtogram of different Power Quality Events

NCT can be extended for Power Quality (PQ) analysis by applying it to the analysis of PQ signals. PQ analysis involves the assessment of various electrical parameters to evaluate the quality and reliability of electric power. As per the Fig. 6 it is evedent that each power quality events have its own features which can be extracted by the propsedmeythodology. The SpectrulKurtogram (SK) of each events determine its frequency distribution at different level of its decomposition. As per the binary tree[32] decomposition of the SK determine the signature charecteristics of all type of PQ events.

Classifier

The classes are labeled as C

F1-voltage fluctuation

F2-voltage fluctuation with harmonics

F3 – voltage fluctuation with transient,

F4 – voltage interruption, C5 – sag

F6 – swell,

F7 – harmonics,

F8 – oscillatory transients,

F9 – notch,

F10 – spike,

F11 – sag with harmonics,

F12 – swell with harmonics,

F13 – sag with transient

F14 – swell with transient

Multi-Class SVM Classifier

The selection of the NCT parameters can be performed using an algorithm that considers the specific requirements and characteristics of the signal being processed. Here's a general algorithm for selecting the parameters in NCT:

Define the objectives: Determine the specific objectives you want to achieve with NCT. This could be signal compression, denoising, feature extraction, or any other desired signal processing task.

Based on the given input signal X(n) and a set of candidates $r \in [rlow : \tau r : rup]$, where τr is the step size of r, the following iterative procedure can be followed to determine the appropriatecombination with the maximum score:

1. Set J = np, where np is the number of main peaks in the spectral magnitude of X(n).
2. Iterate over each candidate value of r from rlow to rup with a step size of τr.
3. For each r value, compute the parameter Q using the equation specified in (8).
4. Use the obtained values of (r, Q, J) to decompose the input signal X(n) using the NCT (Time-Varying Wavelet Transform) technique.
5. Compute the SAEWSE for the current (J, Q, r) combination using Equation (6).
6. Repeat steps 3-5 for all candidate r values.
7. Determine the δ_λ and $\xi_\lambda$value in NCT combination that yields the maximum SAEWSE.

By following this iterative procedure, you can find the appropriateδ_λ and $\xi_\lambda$value in NCT combination that maximizes the score, which can be used for further analysis or processing of the input signal.The functions f1(W) and f2(W) are grid-like structures built in two dimensions. The extent of this grids is the same as that of the data set. After that, we assign each grid cell a U value. All data values "near" this grid point were averaged to arrive at this U value. We use this averaged knowledge to build the 3D surface. Consequently, the

Here, $\sum b_i$ represents the summation of all points in Set B.

These expressions represent the centroid or 'centre of mass' of each set, which gives an approximate central point for the respective set of points in N-dimensional space.

Inding a hyperplane that separates the two sets of points in N-dimensional space. Let's summarize the steps:

1. **Compute the Centres of Mass**: Calculate the 'centres of mass' for both sets of points. For Set A with K points {ai}, the centre of mass is A, and for Set B with S points {bi}, the centre of mass is B.
2. **Compute the Mid-Point**: Find the mid-point between the two centres of mass, which will serve as a point on the hyperplane. This point is denoted as M.
3. **Compute the Normal Vector**: Calculate the vector C by subtracting B from A. This vector will serve as the normal vector to the hyperplane.
4. **Normalize the Normal Vector**: To ensure that the normal vector is a unit vector, normalize it by dividing it by its magnitude. The normalized vector is denoted as n^.
5. **Find a Basis for the Hyperplane**: To represent points on the hyperplane, you need N-1 orthogonal vectors that lie in the (N-1)-dimensional hyperplane. These vectors can be obtained using a Gram-Schmidt type process, starting with a trivial basis and ensuring that each new vector is orthogonal to all the previous ones and orthogonal to the normalized normal vector, n^.
6. **Represent Points on the Hyperplane**: Any point on the hyperplane can be represented by N-1 coordinates αi (for I = 1 to N-1). These coordinates correspond to a point in the original N-dimensional space and can be calculated using the basis vectors obtained in the previous step.

   The final expression for a point q on the hyperplane is given by: q = Σ(αj ×vj) + M

   Where Σ denotes summation over j = 1 to N-1, and vj represents the N-1 basis vectors obtained using the

SVM was developed by Vapnik et al. and is grounded in statistical learning theory, particularly Vapnik-Chervonenkis theory. This theory deals with the capacity of a learning algorithm to generalize from the training data to unseen data, which is crucial for effective machine learning. VM is effective in dealing with linearly inseparable input data by mapping it to a higher-dimensional feature space. This nonlinear feature mapping is achieved using a kernel function, denoted as K(ui, uj), which transforms the original data points into a space where they can be linearly separated.In the high-dimensional feature space, SVM constructs a linear hyperplane that separates the data points belonging to different classes. The goal is to find the optimal hyperplane that maximizes the margin between the classes. The margin is the distance between the optimal hyperplane and the data points closest to it, known as the bounding planes. By finding the optimal hyperplane with a maximum margin, SVM aims to minimize the chances of misclassification. A larger margin allows for better generalization and improves the classifier's ability to classify unseen data accurately. The expression calculates the 'centres of mass' for the two sets of points in N-dimensional space. Let's break down the computation for both sets:

1. For Set A: The set A consists of K points in N-dimensional space: {a1, a2, ..., ak}. To find the 'centre of mass' for this set, we calculate the average of all the points in the set.

   Centre of Mass for Set A (A_mean): A_mean = $\frac{1}{K} \times \sum a_i$

   (for i= 1 to K)

   Here, $\sum a_i$ represents the summation of all points in Set A.

2. For Set B: The set B consists of S points in N-dimensional space: {b1, b2, ..., bs}. To find the 'centre of mass' for this set, we calculate the average of all the points in the set.

   Centre of Mass for Set B (B_mean): B_mean = $\frac{1}{S} \times \sum b_i$

   (for i= 1 to K)

food, encapsulating food, and oscillating, which can be represented as follows:

Approach food

Decision Tree classifier

Based on the provided information, the paper uses a Multiclass Support Vector Machine (MSVM) classifier to create an initial rule-based decision tree for classifying power quality (PQ) disturbances. The construction of the decision tree is based on the standards and definitions of PQ disturbances as referenced in [1] and [30]. These standards likely provide guidelines and criteria for categorizing different types of PQ disturbances.

Once the initial decision tree is constructed, it undergoes a refinement process based on the analysis of training patterns. This refinement process aims to improve the accuracy and performance of the decision tree classifier. The specific details of the refinement process might involve pruning, splitting nodes, or other techniques to optimize the decision tree structure for better classification.

As a result of this refinement, the paper claims to achieve an optimal decision tree, which is efficient in classifying eight single PQ disturbances labeled as F1 and C4 to F10. The PQ disturbances are likely categorized into different classes based on the specific types and characteristics of each disturbance.Figure8 in the referenced document is expected to show the structure or visualization of this optimal decision tree. The figure might illustrate the branching and decision-making process of the tree, showing how the classifier distinguishes and assigns incoming data patterns to different classes of PQ disturbances.Overall, the proposed approach seems to integrate the NCT-based feature extraction with the MSVM classifier and an optimized decision tree to achieve accurate and efficient classification of various PQ disturbances. The use of standardized definitions and a refinement process helps enhance the performance of the classifier, making it suitable for real-world power quality analysis.To gain a deeper understanding of the methodology and results, referring to the specific referenced documents [1], [30], Gram-Schmidt process. The point q lies on the N-dimensional hyperplane defined by the two sets of points A and B in N-dimensional space.

The feature selection and parameter optimization approach using SMA-SVM

SVM classifier accuracy and computation efficiency may be enhanced by minimizing the amount of features included in the model and by adhering to strict accuracy requirements during fitness function design. In other words, the fitness value increases as the number of features decreases and the classifier's classification accuracy improves [27]. In this research, we build the chromosomal fitness function using the weighted classification accuracy and weighted features of SVM, as given in the formula **(9).**

The proposed SMA-based technique and the tried-and-true Grid methodology

Our procedures involve the development of two object functions: the first characterizes the performance of the support vector machine (SVM) in classifying data, and the second characterizes how to choose features using the Slime MouldAlgorithm(SMA).

The fitness function incorporates a weighted combination of the two criteria. The user is able to adjust the weight.

$$\text{Fitness}=W_A\times\text{SVM\_Accuracy}+W_F\times\left(\sum_{i=1}^{nf} C_i \times F_i\right)^{-1}$$

W_A= Accuracy weight of SVM classification

SVM_Accuracy=Classification Accuracy

W_F= Weight of number of features

C_i= Cost of the feature i

F_i= '1' represents that feature i is selected; '0' represents that feature i is not selected

Li Shimin et al. proposed the SMA which has been inspired from the behavioural aspect of slime mould [27]. In the nature, the slime mould detects the food and thereafter encircles it and eventually digest it by releasing enzymes. The properties of slime mould may be mathematically expressed into three steps: seeking

be thought of as a group because their shared TF4 characteristic is so similar. Sag, sag with harmonics, and sag with transients are all distributed along the TF4 axis since they all have the same sag depth of 0.1 to 0.9 pu.

For the experimental verification of the proposed method in hardware platform, the authors have fed the bus distribution system in the RTDS system. The considered model is simulated in PSimand the simulation have been carried out by utilizing Opal-RT RTS OP5600 chassis with RT lab form of 11.X. Voltage signals consequently produced by Opal-RT real-time test system, have been sent to IO cards ML605 is used to gather the required information.Finally, an OROS-34 data acquisition card (DAQ) samples a current signal from a laboratory setup at 12.8 kHz, as illustrated in Fig. 10, and the suggested approach is evaluated on this signal. The scene opens with a mobile phone and laptop being charged, followed by the activation of a personal computer. This load change resulted in a transient lasting for around 1.6 ms with an intensity about three times that of the signal amplitude.

Conclusions

The proposed automatic technique for recognizing Power Quality (PQ) disturbances presents a comprehensive approach that combines various advanced techniques to achieve accurate and efficient detection and classification. Here are the key points that enhance the recognition capability of PQ disturbances. The NCT is used to extract the actual fundamental frequency component from the input signal. This step ensures accurate decomposition and isolation of the fundamental frequency, which is vital for distinguishing different types of PQ disturbances. By focusing on the fundamental frequency component, the method can effectively separate it from other harmonics and interharmonics..

REFERENCES

[6] R. C. Dugan et al., Electrical Power Systems Quality. New York, NY, USA: McGraw-Hill, 2012.

[7] J. V. Milanovic et al., “International industry practice on power-quality monitoring,” IEEE Trans. Power Del., vol. 29, no. 2, pp. 934–941, Apr. 2014.

[8] M. Kezunovic and Y. Liao, “A novel software implementation concept for power quality study,” IEEE Trans. Power Del., vol. 17, no. 2, pp. 544–549, Apr. 2002.

[9] M. A. S. Masoum, S. Jamali, and N. Ghaffarzadeh, “Detection and classification of power quality disturbances using discrete wavelet transform and

and [31] would provide more detailed insights into the standards used, the decision tree refinement process, and the visualization of the optimal decision tree structure

Result Analysis

A total of 5000 signals were collected for this study, with 300 representing each of the 14 power quality (PQ) disturbances and 800 serving as test signals. The disturbance signals are realistic in that they include fundamental frequency fluctuations of 0.2 Hz and variable phase angles. Signals are generated in MATLAB using standards and specifications [25, 30] to guarantee conformity with industry norms.nA 6 kHz sampling rate and a 0.2s sliding window are used to capture each time-varying waveform. To evaluate the robustness of the proposed approach against noise interference, the produced signals are contaminated with noise. From -20 dB to -50 dB, the signal-to-noise ratio (SNR) accommodates a range of background noise densities.For each category of PQ disturbances, the dataset is split in half, with one half used for training and the other for validation. For uniform analysis, the input signals are normalized to 1 per unit (pu).Current signals with harmonics, interharmonics, transients, and voltage disturbances are the focus of this research.A significant factor in the assessment is frequency-related distortions, which are prevalent noise sources in modern communications.$Accuracy_j = C_{Nj}\ T_{Nj} \times 100$ (19)

Where C_{Nj} is the number of signals in class j that were successfully identified and T_{Nj} is the total number of test signals in class j.

Identification of Power Quality Disturbances

A final feature vector including T1, T2, and T3 is supplied as input to the first MSVM for classification of 3 disturbances (F1 - C3) in the instance of voltage fluctuation signals.Figure 8 shows a scatter plot of these PQ disturbances in feature space, demonstrating that they can be reliably differentiated from one another regardless of the features used. Therefore, it is not surprising that the first MSVM's classification accuracy is also 100%. In the absence of any other low-frequency Using all five characteristics as inputs, the second MSVM is picked for interharmonics. T1, T3, and T4 feature space scatter plot of 14 PQ disturbances is In order to see the progression of disturbances clearly, a logarithmic scale is used for the graphic. The graphic clearly shows how the interruption, harmonics, and transients may be isolated from one another. When compared in these three dimensions, notches and spikes reveal striking similarities.As a result, they share the same set of features indistinguishably. Also, swell, swell with harmonics, and swell with transient may

[2] A. Abdelsalam, A. A. Eldesouky, and A. A. Sallam, "Characterization of power quality disturbances using hybrid technique of linear Kalman filter and fuzzy-expert system," Elect. Power Syst. Res., vol. 83, no. 1, pp. 41–50, 2012.

[3] Bracale, P. Caramia, and G. Carpinelli, "A new, sliding-window Prony and DFT scheme for the calculation of power quality indices in the presence of non-stationary disturbance waveforms," Int. J. Emerg. Elect. Power Syst., vol. 13, no. 5, Dec. 2012.

[4] Bracale, G. Carpinelli, I. Y.-H. Gu, and M. H. J. Bollen, "A new joint sliding-window ESPRIT and DFT scheme for waveform distortion assessment in power systems," Elect. Power Syst. Res., vol. 88, pp. 112–120, Jul. 2012.

[5] W. Chang and C.-I. Chen, "Measurement techniques for stationary and time-varying harmonics," in Proc. IEEE PES Gen. Meeting, Minneapolis, MN, USA, 2010, pp. 1–5.

wavelet networks," IET Sci. Meas. Technol., vol. 4, no. 4, pp. 193–205, Jul. 2010.

[10] P. K. Ray, N. Kishor, and S. R. Mohanty, "Islanding and power quality disturbance detection in grid-connected hybrid power system using wavelet and S-transform," IEEE Trans. Smart Grid, vol. 3, no. 3, pp. 1082–1094, Sep. 2012.

[11] S. He, K. Li, and M. Zhang, "A real-time power quality disturbances classification using hybrid method based on S-transform and dynamics," IEEE Trans. Instrum. Meas., vol. 62, no. 9, pp. 2465–2475, Sep. 2013.

[12] S. Mishra, C. N. Bhende, and B. K. Panigrahi, "Detection and classification of power quality disturbances using S-transform and probabilistic neural network," IEEE Trans. Power Del., vol. 23, no. 1, pp. 280–287, Jan. 2008.

[1] S. Shukla, S. Mishra, and B. Singh, "Empirical-mode decomposition with Hilbert transform for power-quality assessment," IEEE Trans. Power Del., vol. 24, no. 4, pp. 2159–2165, Oct. 2009.